Received: 24 November 2021 | Revised: 17 March 2022 | Accepted: 20 March 2022

DOI: 10.1002/bit.28093

ARTICLE

BIOTECHNOLOGY AND BIOENGINEERING WILEY

Continuous countercurrent chromatographic twin-column purification of oligonucleotides: The role of the displacement effect

Ismaele Fioretti[1] | Thomas Müller-Späth[2] | Richard Weldon[2] | Sebastian Vogg[2] | Massimo Morbidelli[1] | Mattia Sponchioni[1]

[1]Department of Chemistry, Materials and Chemical Engineering, Politecnico di Milano, Milano, Italy

[2]YMC ChromaCon, Zürich, Switzerland

Correspondence

Mattia Sponchioni, Department of Chemistry, Materials and Chemical Engineering, Politecnico di Milano, Via Mancinelli 7, Milano, 20131, Italy.
Email: mattia.sponchioni@polimi.it

Funding information

YMC Japan

Abstract

Oligonucleotides (ONs) are breaking through in the biopharmaceutical industry as a promising class of biotherapeutics. The main success of these molecules is due to their peculiar way of acting in the cellular process, regulating the gene expression and hence influencing the protein synthesis at a pretranslational level. Although the Food and Drug Administration (FDA) already approved a few ON-based therapeutics, their production cost strongly limits large-scale manufacturing: a situation that can be alleviated through process intensification. In this study, we address this problem by developing an efficient and continuous chromatographic purification process for ONs. In particular, we considered the chromatographic purification of an ON crude prepared by chemical synthesis using anion exchange resins. We demonstrate that in this system the competitive adsorption of the various species on the same sites of the resin leads to the displacement of the more weakly adsorbing species by the more strongly adsorbing ones. This phenomenon affects the behavior of the chromatographic units and it has been investigated in detail. Then, we developed a continuous countercurrent solvent gradient purification (MCSGP) process, which can significantly improve the productivity and buffer consumption compared to a classical single-column, batch chromatographic process.

KEYWORDS

chromatography, continuous, displacement, MCSGP, oligonucleotides

1 | INTRODUCTION

During the last decades many biopharmaceuticals, in particular monoclonal antibodies and peptides, have been developed and entered the market or clinical trials (Catani et al., 2020; Glennie & Johnson, 2000). Despite their success, these types of molecules suffer from some limitations. Particularly, their pharmacokinetics is often unsatisfactory, since the fraction of the dose which eventually interacts with the target may be as low as 20% (Chames et al., 2009). In addition, since they act in the cellular process after the protein translation in the ribosomes, problems may occur particularly in the case of patients with degenerative diseases (Nelson et al., 2010). This

is the main reason why a drug that intervenes in an earlier step of the protein synthesis represents a very promising innovation. This is the case of oligonucleotides (ONs) (Andersson et al., 2018; Enmark et al., 2020; Morrison, 2019; Yin & Rogge, 2019), which act at a pretranslational level (Gold, 1995), and are able to act through either silencing or modifying the gene expression, instead of acting on the expressed proteins (Bilanges & Stokoe, 2005; Chen et al., 2005; Gooding et al., 2016; Kazutaka et al., 2016; Roberts et al., 2020).

Nowadays, few ON-based drugs have been approved by the Food and Drug Administration (FDA) (Ginn et al., 2018; Ho & Yu, 2016; Hoy, 2018; Keam, 2018; J. Kim et al., 2019; Stein & Castanotto, 2017). The manufacturing is mostly based on phosphoramidite-based solid-phase synthesis (Paredes et al., 2017), which leads to a solution of the target compound mixed with many structurally similar impurities. These are shortmers (i.e., $n-1$, $n-2$, etc.) or longmers (i.e., $n+1$, $n+2$, etc.), which, due to the molecular similarity to the product, are very difficult to separate. Accordingly, the downstream purification of these crudes is quite challenging and typically adsorbs a good fraction of the production cost (Capaldi et al., 2017; El Zahar et al., 2018).

In this study, we show how chromatographic processes can be designed and adopted for this purification and how their efficiency can be highly increased by using continuous countercurrent operations. In particular, we show that, at least in the case of the chromatographic purification of ONs considered in this study, the so-called *displacement effect* characterizes the separation of the target product from the corresponding impurities. This effect has been described in the past for systems under overloaded conditions (Carta & Jungbauer, 2010; Seidel-Morgenstern, 2004), but is here reported for the first time for ONs. In a multicomponent mixture, the displacement effect takes place when the different species in the mixture compete for the same adsorption sites on the chromatographic resin. This typically occurs at high loadings, since in dilute conditions the different species do not compete and therefore the system is well described by linear equilibrium isotherms (Eble et al., 1987; Golshan-Shirazi & Guiochon, 1990; Guiochon & Ghodbane, 1988; Guiochon & Katti, 1987). The physical explanation of the displacement effect can be easily made considering a binary mixture, where the second component exhibits the highest affinity to the resin. Once the first component is adsorbed and the active sites of the resin get close to saturation, the second component starts competing with it for a binding site, and eventually replaces it by desorbing it back to the liquid phase. This is reflected in the shape of the elution chromatograms, where for increasing loadings the peak shape of the second component becomes steeper in the front due to the Langmuir adsorption behavior that this ONs follow when the column is overloaded (Horvath et al., 1981; Kalász, 2003). In the case of a single-column batch chromatography, this peculiar behavior can be exploited to improve the purification performance in terms of purity and yield, as the displaced component elutes earlier or can even be pushed in the washing phase before the elution, thus increasing the resolution of the separation. In this study, we investigate how the displacement effect is affected by some relevant operating conditions, such as loading, the modifier gradient, and the particle size of the resins.

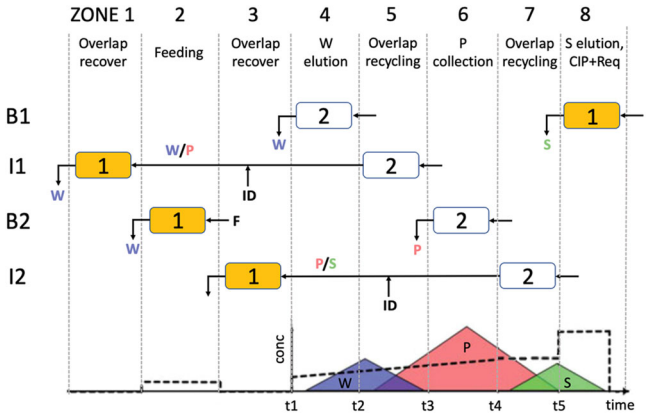

FIGURE 1 Scheme of the MCSGP mode of operation during one switch. The gray dashed vertical lines indicate the eight different tasks executed during the process divided into four steps (B1, I1, B2, and I2). B1 is the first batch phase, I1 the first interconnected phase, B2 the second batch phase, and I2 is the second interconnected phase, The five time points $t1$–$t5$ are the ones to be set during the MCSGP operation design. $t1$ is the start of the weakly adsorbing impurity W elution, $t2$ is the end of the weakly adsorbing impurity elution and the start of the W/P recycling portion, $t3$ is the end of the W/P recycling region and the start of the product P collection, $t4$ is the end of the P collection and the start of the P/S recycling portion, and $t5$ is the end of the P/S recycling region.

Next, we translate the process from batch to a continuous countercurrent operation using the multicolumn countercurrent solvent gradient purification process (MCSGP). Since the concept behind this process and the operation of the corresponding unit has been already described in detail (Aumann & Morbidelli, 2007, 2008; Baur et al., 2016; Bigelow et al., 2021; Jungbauer, 2013; T.K. Kim et al., 2021; Krättli et al., 2013; Luca et al., 2020; Müller-Späth et al., 2013; Steinebach et al., 2016; Ströhlein et al., 2006; Ulmer et al., 2017; Vogg et al., 2020), here we briefly recall only the basic concepts.

Considering the typical chromatogram of a central-cut purification illustrated in Figure 1, the general idea of the MCSGP consists in collecting the target product (P), characterized by a purity above the specification limit, while recycling the overlapping peaks in the front and in the back, characterized by weakly adsorbing impurities co-eluting with the product (W/P) and strongly adsorbing impurities co-eluting with the product (P/S), respectively. The first switch of this cyclic operation occurs between the upstream column (column 2 in Figure 1), in which the elution takes place, and the downstream column (column 1 in Figure 1), in which the recycling portions from the upstream column are readsorbed. At the end of the first switch, the columns exchange the position, and the process is repeated completing the

first cycle. Each single switch can be then divided into four steps as indicated in Figure 1:

- The first batch phase (B1), where the elution of the weakly adsorbing impurities takes place in the upstream column, while the downstream column is cleaned and re-equilibrated.
- The first interconnected phase (I1), where the overlapping peaks W/P are recycled, after appropriate inline dilution (ID) to restore binding conditions, from the upstream to the downstream column.
- The second batch phase (B2), where the product collection is performed in the upstream column, while the downstream column is loaded with fresh feed.
- The second interconnected phase (I2), where the overlapping peaks P/S are recycled after an appropriate inline dilution, similarly as in phase I1.

The proper design of the operating conditions of an MCSGP is more difficult than for a batch process because of the larger number of degrees of freedom. In addition to the operating parameters to be considered in a standard single-column process and to the characteristic times of the product elution window (see times $t3$ and $t4$ in Figure 1), other three characteristic times have to be set: $t1$ as the start of the weakly adsorbing impurity elution, $t2$ to set the start of the W/P recycling portion, and $t5$ to stop the P/S recycling. At $t4$, the linear gradient operation is replaced by an isocratic operation until $t5$. At $t5$ a step change in the buffer composition is implemented to perform cleaning-in-place (CIP) and strip all the remaining impurities adsorbing to the column. The correct setting of these five times is essential to maximize the product yield and to avoid the impurity accumulation inside the column so as to reach satisfactory steady-state conditions. Given their importance on the outcome of the process, preliminary batch experiments with off-line analysis of the fractions collected during the elution phase are essential to determine the product profile and hence to accurately set the product collection window as well as the recycling intervals.

Another aspect to consider is the inline dilution that takes place two times per switch and heavily influences the final productivity that can be obtained with the process. In fact, the dilution factors have to be set to ensure binding conditions in the downstream column during the two interconnected phases by reducing the concentration of the modifier in the recycling fractions to the value at the beginning of the gradient. The flow rate in the recycling phases should then be tuned accordingly, so that the flow rate of the diluent combined with the one of the recycling portions does not overcome the maximum pressure sustainable by the downstream column. This typically requires a reduction in the recycling flow rate, especially in the interval $t4$–$t5$ (P/S recycling) where the dilution factor is high.

After having highlighted the role played by the displacement effect in the purification of an ON sequence with a single-column batch operation, we discuss the design of the MCSGP process focusing attention on how this displacement effect can be advantageously exploited to improve its performances when operating at high loadings.

2 | MATERIALS AND METHODS

2.1 | Materials

The ON used in this study consists of a 20mer single-strand DNA sequence kindly provided by YMC Japan.

The equilibration buffer used in the analytical method is 100 mM hexafluoro-2-propanol (HFIP, ≥99%, MW = 168.04; Sigma-Aldrich) and 4 mM triethylamine (TEA, ≥99%, MW = 101.19; Thermo Fisher). The elution buffer used in the analytical method is methanol (≥99.9%, MW = 32.04; Sigma-Aldrich). The equilibration buffer used in preparative chromatography is 20 mM sodium hydroxide (NaOH, ≥99%, MW = 40.00; Sigma–Aldrich), while the elution buffer is 20 mM NaOH and 1.2 M sodium chloride (NaCl, ≥99%, MW = 58.44; Sigma-Aldrich). Deionized water (DW) (Merck Millipore) is used for buffer preparation. All buffers are filtered with 0.44 µm cellulose-acetate filters (Merck Millipore) and degassed for chromatographic purposes.

2.2 | The analytical chromatographic method

The crude as well as all the samples collected from the elution stream were analyzed via reverse phase ultrahigh-performance liquid chromatography (RP UHPLC). The analytical experiments were run with a YMC Triart C18 resin using an Agilent Infinity II 1290 UHPLC. The adopted method for the sample analysis is reported in Table 1.

TABLE 1 Analytical reverse phase ultrahigh-performance liquid chromatography method.

	Resin: YMC—Triart C18, S—1.9 µm, 12 nm
Column dimension (ml)	0.314 (100 × 2 mm)
Feed concentration (g/l)	4.775
Sample dilution	Step 1—2:1 in 10 mM acetic acid/ Step 2—1:1 in HPLC grade H_2O
Buffers	Equilibration buffer: 100 mM HFIP + 4 mM TEA Elution buffer: methanol
Injection volume (µl)	0.5
Flow rate (ml/min)	0.2
Equilibration duration (5% B) (min)	1
Gradient	1–3 min (5%–10% B), 3–20 min (10%–20% B), 20–22 min (20%–90% B)
Strip duration (90% B) (min)	1
Reequilibration duration (5% B) (min)	20

TABLE 2 Operating parameters of the batch experiments with resin BioPro IEX SmartSep Q30 and Q75.

	Batch operation—Resin BioPro IEX SmartSep
Column dimension (ml)	2.1 (0.5 × 10.6 cm)
Buffers	Equilibration buffer: 20 mM NaOH Elution buffer: 20 mM NaOH + 1.2 M NaCl
Loading flow rate (cm/h)	300
Equilibration (10% B) flow rate (cm/h)	450
Equilibration duration (CV)	2
Wash (10% B) flow rate (cm/h)	300
Wash duration (CV)	3
Gradient flow rate (cm/h)	150
Gradient duration (CV)	10
Strip (100% B) flow rate (cm/h)	450
Strip duration	2
Re-Equilibration (10% B) flow rate (cm/h)	450
Re-Equilibration duration (CV)	3
Particle size Q30 (μm)	30
Particle size Q75 (μm)	75
Resin loading Q30 (g/L)	3.5; 10; 20
Resin loading Q75 (g/L)	20; 30
Gradient %B Q30 (%)	15–80; 10–80
Gradient %B Q75 (%)	10–80

The absorbance was measured at 260 nm with a diode-array detector and the separation was conducted at 50°C.

2.3 | The batch operation

The equipment used to perform the preparative chromatography is a Contichrom CUBE (YMC ChromaCon), using a BioPro IEX SmartSep resin (YMC Japan). The chromatogram is recorded by measuring the UV absorbance at 280 nm. The operating parameters used for the different single-column batch experiments discussed in this study are summarized in Table 2. Three operating parameters were varied: the feed loading, the gradient boundaries and, the particle size of the resins.

The characterization of the fractions collected during the elution phase of the batch experiment with load of 10 g/L, gradient boundaries 15%–80% B and particle size 30 μm and based on the results of RP UHPLC is reported in Table S1 as an example. The process performance is then evaluated in terms of purity, yield, productivity, and specific buffer consumption. The purity is given by the ratio between the area of the target product ($Area_{target}$) and the total area of the chromatogram ($Area_{total}$), as indicated in Equation (1):

$$\text{Purity} \quad (\%) = \frac{Area_{target}}{Area_{total}} \times 100. \tag{1}$$

The yield, referred to the target component, is given by the ratio of the recovered target product mass ($m_{recovered}$) and the total amount of product loaded in the column (m_{total}):

$$\text{Yield } (\%) = \frac{m_{recovered}}{m_{total}} \times 100. \tag{2}$$

The process productivity, for a given total duration of the experiment (t) and column volume (CV), is given by

$$\text{Productivity } (g/L/h) = \frac{m_{recovered}}{CV \times t} \tag{3}$$

Finally, the specific buffer consumption is calculated as the ratio between the volume of the consumed buffers (V_{buffer}) per mass of purified product:

$$\text{Buffer consumption } (L/g) = \frac{V_{buffer}}{m_{recovered}}. \tag{4}$$

Finally, the process mass intensity (PMI) is also calculated as an index of the overall process efficiency of the manufacturing process, specifically with respect to its environmental impact. This is given by the ratio between the total input mass to the process (buffers, raw material, and resin) ($mass_{process}$) and the mass of purified product (Cataldo et al., 2020; Madabhushi et al., 2018), as indicated in Equation (5):

$$\text{PMI } (g/g) = \frac{m_{process}}{m_{recovered}}. \tag{5}$$

An example of calculation of these performance parameters is reported in the Supporting Information section with reference to the process conditions reported in Table S2.

Out of the different fractions collected during the elution phase of the batch experiment, different hypothetical pooling windows were considered by proper fraction aggregation, with the performance parameters for each pooling window reported in Table S3. From these, it is possible to experience the mentioned trade-off between yield and purity observed when modulating the duration of the product collection window, which is a major limitation of single-column operations.

2.4 | The MCSGP operation

The MCSGP experimental runs are designed starting from the corresponding batch chromatogram. Using the chromatogram

obtained with the single-column run at 10 g/L loading, the recycling windows and the product collection window are set by fixing the five time points $t1$–$t5$. The amount of crude fed in each cycle is computed to replace the product collected in the product elution window (PEW) of the previous cycle. The loading flow rate for the MCSGP is selected to match, with the loading time, the time required for eluting the product from the upstream column. In fact, these two steps occur concomitantly in the two involved columns. This typically leads to lower loading flow rates compared to batch, which in turn allows higher residence time of the ON. The two inline dilution (ID) factors are calculated to bring the salt concentration in the downstream column back to the starting condition of the gradient. The flow rate of the diluting buffer is then set as to ensure the required dilution factor to the eluent from the upstream column, whose flow rate is constant to 150 cm/h for the whole elution phase. The values of the operating parameters of the experimental runs are summarized in Table 3.

The off-line characterization of the product pools collected during the different MCSGP cycles is reported in Table S4 for the experimental Run 1 as an example. The process performance for the different experimental runs is evaluated, similarly to the batch runs, in terms of purity, yield, productivity, and specific buffer consumption based on the process parameters summarized in Table S5. The purity obtained in each cycle of the MCSGP run is calculated as in Equation (6):

$$\text{Purity} \quad (\%) = \frac{\sum_1^n \text{Area}_{\text{target}\_i}}{\sum_1^n \text{Area}_{\text{total}\_i}} \times 100, \tag{6}$$

where A_{target_i} is the area of the target product in the PEW fraction of cycle i, A_{total_i} is the total area of the PEW fraction of the cycle i, and n is the total number of cycles. The yield can be expressed as the ratio between the sum of the recovered product masses collected during each cycle in the product fraction ($m_{\text{recovered}\_i}$) and the sum of the product masses loaded in the column for each cycle (m_{total_i}) as in Equation (7):

$$\text{Yield} \quad (\%) = \frac{\sum_1^n m_{\text{recovered}\_i}}{\sum_1^n m_{\text{total}\_i}} \times 100. \tag{7}$$

The productivity and the specific buffer consumption are calculated according to Equations (8 and 9):

$$\text{Productivity (g/L/h)} = \frac{\sum_1^n m_{\text{recovered}\_i}}{2\text{CV} \times t_{\text{tot}}}, \tag{8}$$

$$\text{Buffer consumption} \quad (\text{L/g}) = \frac{V_{\text{buffer\_tot}}}{\sum_1^n m_{\text{recovered}\_i}}, \tag{9}$$

where t_{tot} is the total duration of the MCSGP experimental run and $V_{\text{buffer\_tot}}$ is the total amount of buffers consumed in the run.

The PMI is also calculated for the MCSGP process and, similarly to the batch one, it is expressed as the ratio between the sum of the total input masses used in each cycle (m_{process_i}) and the sum of the purified product masses collected in each cycle:

$$\text{PMI} \quad (\text{g/g}) = \frac{\sum_1^n m_{\text{process}\_i}}{\sum_1^n m_{\text{recovered}\_i}} \tag{10}$$

It is worth mentioning that at the beginning and at the end of each experimental run, a start-up and a shutdown procedure need to be executed, respectively. In the start-up, the column is fed with the initial batch reference loading to let the unit operate with the desired amount of target product. In the shutdown instead, the last second switch is performed without feeding the downstream column so as to reproduce a simple batch elution in the upstream column. In all cases, these two steps are not included in the process performance calculation, which therefore refers only to the steady-state operation of the process.

TABLE 3 Operating parameters of the multicolumn countercurrent solvent gradient purification process experiments.

	Run 1	Run 2
Column dimension (ml)	2.1 (0.5 × 10.6 cm)	
Resin	BioPro IEX SmartSep Q30	
Buffers	Equilibration buffer: 20 mM NaOH Elution buffer: 20 mM NaOH + 1.2 M NaCl	
Resin loading (g/L)	10	20
Batch purity (%)	94.5	94.5
Batch yield (%)	34.8	42.5
Number of cycles (−)	5	5
Cycle duration (min)	76.8	76.3
Feed concentration (g/L)	4.43	4.12
Feed in startup (CV)	2.07	4.44
Load volume (CV)	0.80	2.08
Loading flow rate (cm/h)	120	170
Gradient boundaries (−)	15% to 80% B	15% to 80% B
Elution flow rate (cm/h)	150	150
Strip (100% B) (CV)	2	2
Strip flow rate (cm/h)	150	230
Re-equilibration (100% A) (CV)	3	3
Re-equilibration flow rate (cm/h)	150	230
Weak recycling ID factor (−)	2.15	3.27
Strong recycling ID factor (−)	2.65	3.67
Weak recycling flow rate (cm/h)	150	150
Strong recycling flow rate (cm/h)	150	150

3 | RESULTS AND DISCUSSION

3.1 | Crude characterization

Before running the purification processes, the ON crude was characterized via RP UHPLC on Triart C18 resin. The corresponding analytical chromatogram is shown in Figure 2, where the area under the peak corresponding to the target product is highlighted in gray. It is seen that the various species are well resolved by the selected analytical method. The purity of the target product was determined to be 72.1%, based on the ratio of the area under peak of the target, eluting at 14.9 min, and the areas of all the peaks. All the impurities were lumped in two pseudo-components: one eluting earlier than the product, and accounting for 24.4% of the crude (hereinafter called weakly adsorbing impurities, W) and the other eluting later than the product, accounting for 3.5% of the total (hereinafter called strongly adsorbing impurities).

3.2 | Displacement effect in batch purification

Various batch preparative purification runs at different feed loadings were performed to investigate the displacement process and its effect on the elution times of the different impurities. In particular, in Figure 3a,b we show two chromatograms obtained under the same operating conditions but different crude loadings, equal to 10 and 20 g/L, respectively. The chromatograms highlight, in addition to the target product (red), four pseudocomponents: three (w1, w2, w3) representing weakly adsorbing impurities (blue) and one (s1) representing strong impurities (green). It is seen that the most abundant species, after the target product, are the weakly adsorbing impurities (w1, w2, and w3), while the strongly adsorbing impurity s1 represents only a minor fraction of the crude. In particular, w1 is well separated from the product, while w2, which is the most abundant one, partially overlaps with the product. This represents a challenge for the separation. If the PEW is in fact taken sufficiently large to include all the product and then have high yield, the purity is necessarily low since also the impurity w2 is collected. On the other hand, high product purities can be obtained only by suitably restricting the PEW, which negatively impacts on the yield. These considerations are at the basis of the purity-yield trade-off typical for central-cut separations using a single column.

The chromatograms reported clearly illustrate the effect of the displacement mentioned above. At lower loadings (Figure 3a) the impurity w1 is completely inside the gradient phase, which goes from 14 to 57 min. On the other hand, for larger loadings (Figure 3b), the product peak moves towards shorter elution times, due to the displacement effect caused by the strong impurities, while for the same reason the weak impurity w1 is pushed in the wash phase before the gradient started, namely from 12 to 18.5 min.

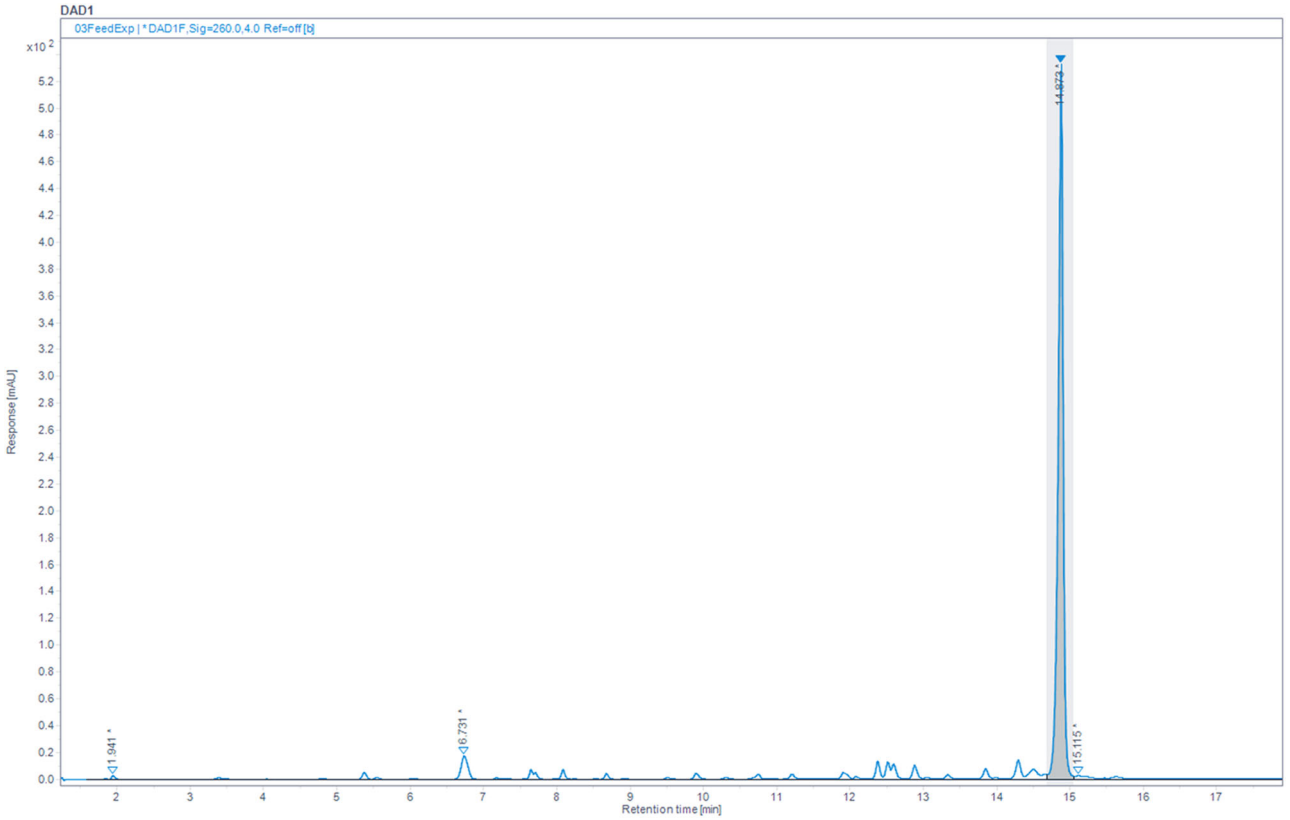

FIGURE 2 Analytical chromatogram of the crude material obtained through reverse phase ultrahigh-performance liquid chromatography on a YMC Triart C18 resin. The gray-colored peak corresponds to the target product; the product purity is 72.1%.

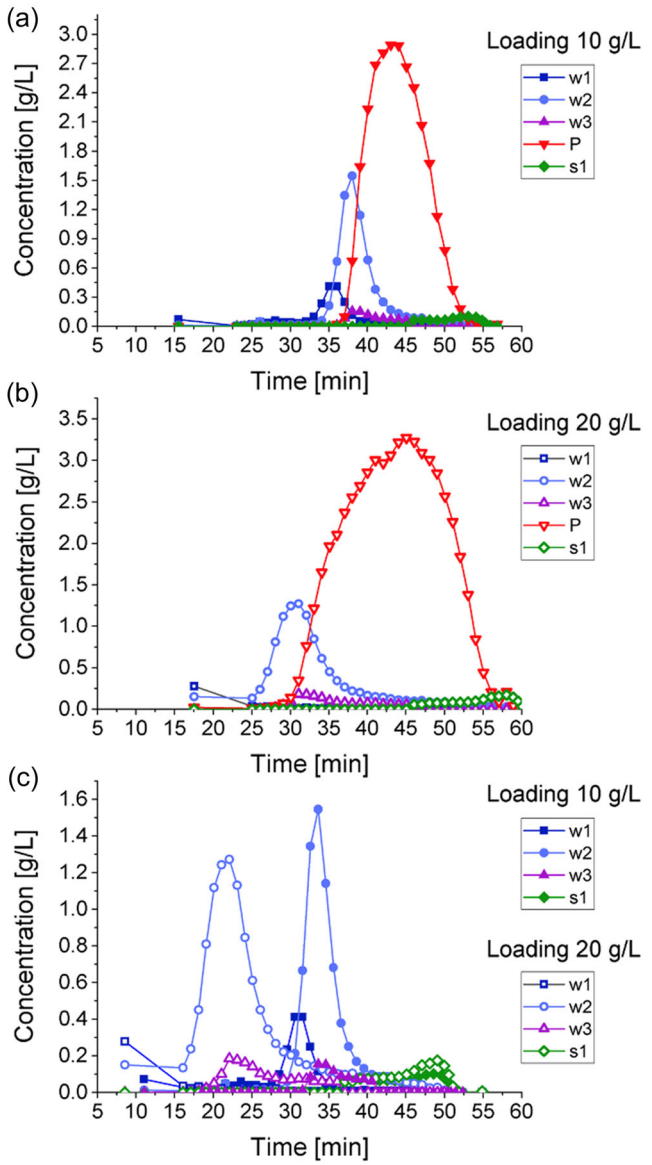

FIGURE 3 Preparative, batch chromatograms with the impurity and the product concentrations obtained from the analytics. The experiment is done with: a particle diameter of the resin of 30 μm, gradient boundaries from 10% to 80% B. w1, w2 and w3 are the three weakly adsorbing impurities, P is the product and s1 is the strongly adsorbing impurity. (a) Loading 10 g/L. (b) Loading 20 g/L. (c) Overlaying of the impurity concentrations from the experiments reported in (a) and (b), for both experiments the loading duration is subtracted from the elution time to better visualize the displacement effect.

To better visualize this effect, in Figure 3c the impurity concentrations measured in the elution phase for the two different loadings are overlapped in the same figure, and the loading duration, which is different for the two cases, is subtracted from both data sets, so as not to affect the elution times of the different species. From this figure it is seen that the three weakly adsorbing impurities are pushed and elute earlier in the case of the larger loading of 20 g/L (see empty symbols in Figure 3c). Interestingly, the elution times of the different species decrease going from 10 to 20 g/L loading proportionally to their affinity to the resin. For example, the retention time of w1 decreases by 71%, while that of w2 and w3, that co-elute with the product, decreases only by 35%. According to the physical principle of the displacement effect, this phenomenon can be exploited to baseline separate the weakly adsorbing impurities in the PEW, without affecting the adsorption behavior of the strongly adsorbing impurities. On the other hand, it is seen that, as expected, the displacement does not affect the elution time of the peak of the strong impurity s1, which increases only in height with increasing loadings.

Let us now consider the performance of the batch process in terms of the Pareto curves reflecting the purity-yield trade-off mentioned above. These can be obtained from the chromatograms reported above, for the two loadings, by considering PEWs of different size and computing the corresponding yield and purity. The obtained results, shown in Figure 4a, indicate that the Pareto curve shifts towards higher purities as the loading increases from 10 to 20 g/L, while keeping constant the particle diameter at 30 μm and the gradient boundaries at 10%–80% B. This apparently contradictory result, that is an improvement in the process performance when operating at larger loadings, is actually understood based on the displacement effect mentioned above. At the same time, we observed that, for a loading of 22.5 g/L, some of the product is lost already during the washing phase, leading to a yield loss of 40%, as the resin binding capacity was reached. Therefore, as intuitive, this represents the maximum extent the displacement effect can be exploited for improving the separation performance. In Figure 4b, the same results are considered but for different gradient boundaries at 15%–80% B and increasing the loading now from 3.5 to 10 g/L, and an improvement in the process performance is obtained. A performance improvement, although to a much smaller extent, is also shown in Figure 4c where bigger resin particles with size equal to 75 μm are used with gradient boundaries of 10%–80% B and loadings increasing from 20 to 30 g/L. In particular, we observed that the purity improvement is larger for lower loadings, while the closer we approach the saturation capacity of the resin the smaller such improvement becomes, that is, going from Figure 4b to Figure 4a and to Figure 4c.

These results confirm that the possibility of improving the performance of batch processes by increasing the loading, because of the displacement effect, is a rather general concept, not sensitive to the other operating parameters.

On the other hand, as expected, in Figure 4a,b it is seen that for the conditions corresponding to 10 g/L loading and a particle diameter of 30 μm, the purity increases going from the 10%–80% B to 15%–80% B gradient, as a consequence of the better resolution associated with the shallower gradient. Likewise, the purity drops passing from a particle diameter of 30 to 75 μm (i.e., Figure 4a,c), for constant values of loading (20 g/L) and gradient boundaries (10%–80% B), because of the slower mass transport inside the larger particles. This is correlated to a further distance to be traveled by the molecules inside the bigger particles,

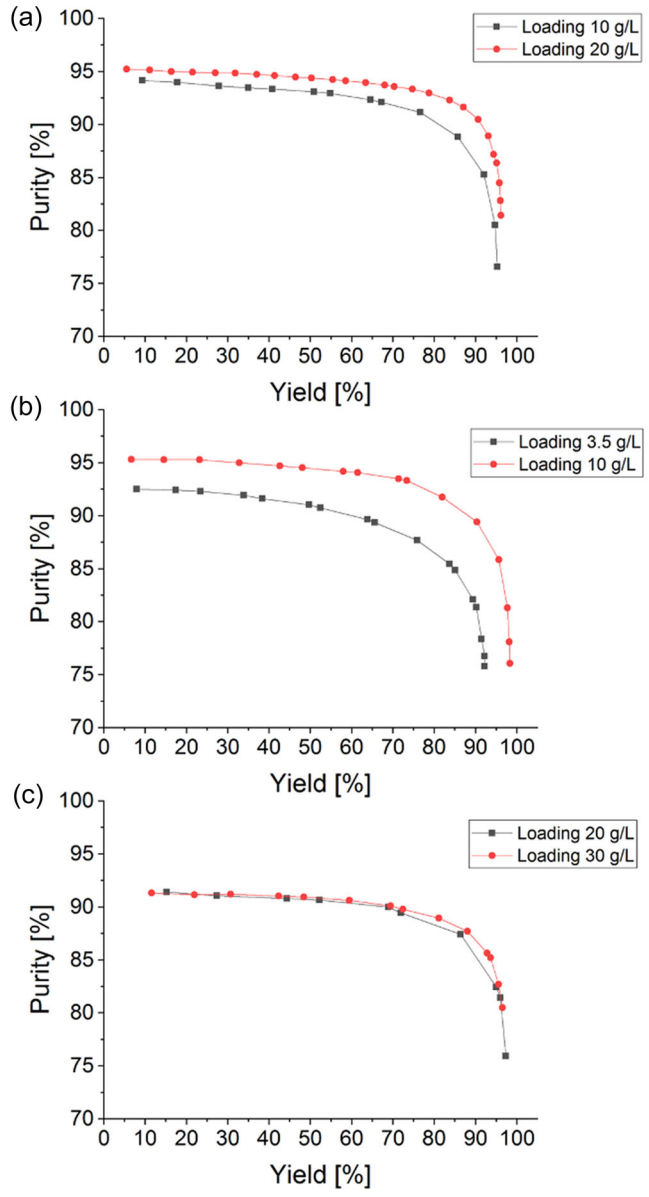

FIGURE 4 (a) Comparison of the Pareto curves purity versus yield for two experimental runs with: same particle diameter 30 µm, same gradient boundaries 10%–80% B and different loadings (10 and 20 g/L). (b) Comparison of the Pareto curves purity versus yield for two experimental runs with: same particle diameter 30 µm, same gradient boundaries 15%–80% B, and different loadings (3.5 and 10 g/L). (c) Comparison of the Pareto curves purity versus yield for two experimental runs with: same particle diameter 75 µm, same gradient boundaries 10%–80% B, and different loadings (20 and 30 g/L).

increasing the dispersion and leading to a peak broadening at the column outlet. These effects are translated into a higher height equivalent to a theoretical plate (HETP), as predicted by the van Deemter's equation and, then, in an overall decrease of the product purity due to an enhanced overlapping between the different species (van Deemter et al., 1995).

3.3 | Displacement effect in MCSGP

After having highlighted the role played by the displacement effect in improving the performances of batch separations, we wanted to investigate how it could be exploited in the case of continuous countercurrent operations. The results of two experimental MCSGP runs at different loadings are shown in Figure 5. These processes were designed to reach a minimum product purity of 95%, which allowed to fix the collection interval *t*3–*t*4 starting from the batch chromatogram. Five cycles were run for each experiment, to reach and confirm steady-state conditions. Each cycle comprises all the batch chromatographic steps (i.e., equilibration, loading, wash, elution, strip) applied twice, once for the first column and once for the second. However, since these steps are partially overlapped in MCSGP, the duration of one cycle is less than two times that of a batch process, as shown in Table 4.

The first experiment was designed based on the batch experiment with 10 g/L loading, gradient boundaries 15%–80% B, and a particle diameter of 30 µm. At steady state, the load of fresh feed per cycle was 3.54 g/L, which reaches the batch loading when the portions that are recycled from the upstream column are added, namely 5.20 and 0.75 g/L loadings for the weak recycling and strong recycling streams, respectively. The corresponding results are shown in Figure 5a,b. In particular, Figure 5a shows the overlapping of the UV signals corresponding to the five performed cycles. It is possible to observe that in this experimental run, the steady state is reached immediately after the first switch of the first cycle, as proved by identical UV profiles obtained from cycle to cycle.

From Figure 5b, comparing the MCSGP performance with the corresponding batch Pareto curve, it is seen that the MCSGP operation significantly improves the performances of the batch process. In particular, the MCSGP leads to a steady-state yield of 92.4% and a product pool purity of 95.4%. The batch purification producing a product pool of similar purity would lead instead to a yield of only 6.6%, which is then improved by 1300% with the continuous countercurrent operation. In addition, the MCSGP performed better than the batch process also in terms of productivity and buffer consumption. In particular, the former increases by 346%, while the buffer consumption decreases by 80% (see detailed values in Table 4). The two processes can be finally compared in terms of PMI, which is a useful green metric for having a clear indication of their environmental footprint. For the batch, the PMI is equal to 51,000 g/g, which gives a clear picture of the resource intensity of this chromatographic operation. Intriguingly, this index can be reduced to 9610 g/g adopting the MCSGP, bringing about a significant advantage of the continuous operation from an environmental point of view.

To demonstrate the role of the displacement effect in a continuous countercurrent operation, a second MCSGP run was carried out, whose loading at steady state was 2.5 times higher (8.55 g/L), under the same gradient boundaries of 15%–80% B. The initial batch loading is reached considering also the recycled feeding

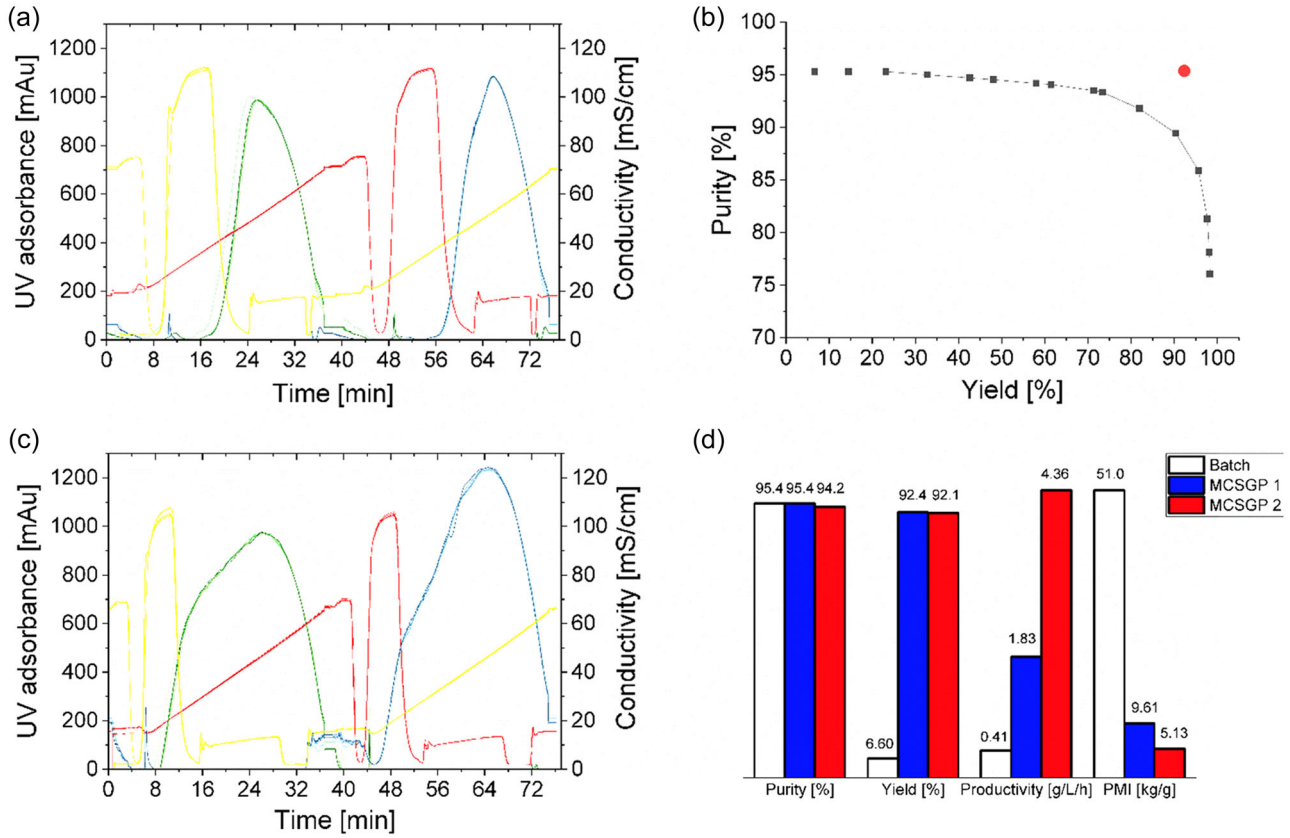

FIGURE 5 First line: Five cycles of the MCSGP run with batch reference loading 10 g/L. (a) UV absorbance and conductivity versus time. The conductivity related to the outlet of the column in position 1 in the Contichrom CUBE is colored in red, while that of the column in position 2 is colored in yellow. The UV signal related to column 1 is colored with a range of greens, while that related to column 2 with a range of blues, depending on the cycle number. (b) The Pareto curve purity versus yield for the batch run with particle diameter 30 µm, 10 g/L loading, and gradient boundaries 15%–80% B is compared with the corresponding MCSGP run (red dot). Second line: Five cycles of the second MCSGP run with elevated loading of 20 g/L. (c) UV absorbance and conductivity versus time. The conductivity related to the outlet of the column in position 1 in the Contichrom CUBE is colored in red, while that of the column in position 2 is colored in yellow. The UV signal related to Column 1 is colored with a range of greens, while that related to column 2 with a range of blues, depending on the cycle number. (d) Histogram showing the performance comparison between the batch run at 10 g/L loading, MCSGP Run 1, and MCSGP Run 2 in terms of purity, yield productivity, and PMI.

streams, equals 8.56 and 1.80 g/L for the weak and the strong recycling portions, respectively. Despite the higher loading that might reduce the process robustness, according to the UV signals shown in Figure 5c, the second MCSGP run reaches the steady-state condition immediately after the first cycle, ensuring constant product quality cycle after cycle. In this case, as shown in Figure 5d and in Table 4, the second MCSGP run leads to a steady-state purity of 94.2% and a yield of 92.1%, comparable to those obtained in the first run with a lower loading. At the same time, the productivity could be improved by 138%. More importantly, the second MCSGP could further reduce the PMI to 5130 g/g, a decrease of 47% with respect to the first run. This is also reflected by the buffer consumption, which is lower for the second MCSGP run, that is 4.74 versus 9.23 L/g (Table 4).

This testifies that the displacement effect is beneficial for improving the separation performance also in the case of continuous operations, allowing the MCSGP to reach higher productivity and reduced environmental footprint by increasing the loading.

4 | SUMMARY AND CONCLUSION

In this study, we investigated the opportunity to improve the ON purification performance through the use of continuous chromatographic processes based on anion exchanging resins. It was found that this system is characterized by the competition of the different species to the same binding sites, which leads to the displacement of the more weakly adsorbing species by the more strongly adsorbing ones. This competitive process has a strong effect on the behavior of the chromatographic purifications and needs to be carefully accounted for.

By first considering a single-column batch process, the effect of increasing loadings on the final purity and yield of the collected target product was investigated. It was found that, in general, the process performance improves for increasing loadings—as it is characteristic for the displacement effect. The role of the resin particle size and the modifier gradient have also been considered. In general,

TABLE 4 Overview of the results of the two MCSGP runs, compared to the corresponding reference batch experiments with the same purity values.

	Batch ref Loading 10 g/L15% to 80%B	MCSGP Run 1	MCSGP Run 2
Product purity (%)	95.4	95.4	94.2
Yield (%)	6.60	92.4	92.1
Product concentration in the eluate (g/L)	1.88	2.10	2.88
Product mass recovery per cycle (mg)	13.8	38.9	92.0
Mass balance (%)	93.4	92.4	92.1
Load per cycle (g/L)	10	3.54	8.55
Loading during W/P recycling (g/L)	-	5.20	8.56
Loading during P/S recycling (g/L)	-	0.75	1.80
Cycle duration (min)	63.7	76.8	76.3
Productivity (g/L/h)	0.41	1.83	4.36
PMI (g/g)	51,000	9610	5130
Buffer consumption (L/g)A	45.3	9.2	4.7

Note: The resin is a BioPro IEX SmartSep Q30, the column volume is 2.1 ml (0.5 × 10.6 cm).

Abbreviation: MCSGP, multicolumn countercurrent solvent gradient purification process.

independently of the operating conditions, it was observed that the purification performance improves with increasing loading, to an extent which decreases as the saturation capacity of the resin is approached.

To improve the performance of the purification process, we transferred the batch process to the continuous countercurrent operating mode using MCSGP. The first MCSGP run was operated for five cycles reaching cyclic steady-state conditions already after the second cycle and showing improvements in terms of purity, yield, productivity, PMI, and buffer consumption over the single-column batch process.

The second MCSGP run was performed with a 2.5 times higher loading for five cycles, and also in this case the process turned out to be robust, with the steady-state condition reached after the first cycle.

By comparing the two MCSGP runs, it was observed that, for similar results in terms of purity and yield, an increased column loading significantly improves the process performance with respect to productivity, buffer consumption and process mass intensity—an important parameter which represents the environmental footprint of the process.

Overall, the MCSGP operated at high loading to exploit the potential of the displacement effect in improving the chromatographic separation is a valuable tool that could reduce the costs associated with the downstream processing of ONs.

AUTHOR CONTRIBUTIONS

Ismaele Fioretti: investigation, validation, writing—original draft preparation. **Thomas Müller-Späth**: funding acquisition (equal), writing—review & edition (equal), supervision. **Richard Weldon**: investigation, methodology. **Sebastian Vogg**: investigation, methodology. **Massimo Morbidelli**1: funding acquisition (equal), writing — review & editing (equal). **Mattia Sponchioni**: supervision, project administration, writing—review & editing (equal).

ACKNOWLEDGMENTS

The authors are grateful to YMC Japan for the financial support. Open Access Funding provided by Politecnico di Milano within the CRUI-CARE Agreement.

CONFLICTS OF INTEREST

The authors declare no conflicts of interest.

DATA AVAILABILITY STATEMENT

Data available on request from the authors

ORCID

Ismaele Fioretti https://orcid.org/0000-0001-9919-6215
Thomas Müller-Späth http://orcid.org/0000-0002-4035-0705
Richard Weldon https://orcid.org/0000-0002-0957-7354
Sebastian Vogg http://orcid.org/0000-0002-6890-6744
Massimo Morbidelli http://orcid.org/0000-0002-0112-414X
Mattia Sponchioni http://orcid.org/0000-0002-8130-6495

REFERENCES

Andersson, S., Antonsson, M., Elebring, M., Jansson-Löfmark, R., & Weidolf, L. (2018). Drug metabolism and pharmacokinetic strategies for oligonucleotide- and mRNA-based drug development. *Drug Discovery Today*, *23*, 1733–1745. https://doi.org/10.1016/j.drudis.2018.05.030

Aumann, L., & Morbidelli, M. (2007). A continuous multicolumn countercurrent solvent gradient purification (MCSGP) process. *Biotechnology and Bioengineering*, *98*, 1043–1055.

Aumann, L., & Morbidelli, M. (2008). A semicontinuous 3-column countercurrent solvent gradient purification (MCSGP) process. *Biotechnology and Bioengineering*, *99*, 728–733.

Baur, D., Angarita, M., Müller-Späth, T., Steinebach, F., & Morbidelli, M. (2016). Comparison of batch and continuous multi-column protein A capture processes by optimal design. *Biotechnology Journal*, *11*, 920–931.

Bigelow, E., Song, Y., Chen, J., Holstein, M., Huang, Y., Duhamel, L., Stone, K., Furman, R., Li, Z. J., & Ghose, S. (2021). Using continuous chromatography methodology to achieve high-productivity and high-purity enrichment of charge variants for analytical characterization. *Journal of Chromatography, A*, *1643*, 462008. https://doi.org/10.1016/j.chroma.2021.462008

Bilanges, B., & Stokoe, D. (2005). Direct comparison of the specificity of gene silencing using antisense oligonucleotides and RNAi. *Biochemical Journal*, *388*, 573–583.

Capaldi, D., Teasdale, A., Henry, S., Akhtar, N., Den Besten, C., Gao-Sheridan, S., Kretschmer, M., Sharpe, N., Andrews, B., Burm, B., & Foy, J. (2017). Impurities in oligonucleotide drug substances and drug products. *Nucleic Acid Therapeutics*, *27*, 309–322.

Carta, G., & Jungbauer, A. (2010). Protein chromatography. WILEY-VCH Verlag GmbH & Co. KGaA, Weinheim.

Cataldo, A. L., Burgstaller, D., Hribar, G., Jungbauer, A., & Satzer, P. (2020). Economics and ecology: Modelling of continuous primary recovery and capture scenarios for recombinant antibody production. *Journal of Biotechnology*, *308*, 87–95. https://doi.org/10.1016/j.jbiotec.2019.12.001

Catani, M., Luca, C. D., Medeiros Garcia Alcântara, J.-o, Manfredini, N.-, Perrone, D., Marchesi, E., Weldon, R., Müller-Späth, T., Cavazzini, A., Morbidelli, M., & Sponchioni, M. (2020). Oligonucleotides: Current trends and innovative applications in the synthesis, characterization, and purification. *Biotechnology Journal*, *15*, 1900226.

Chames, P., Van Regenmortel, M., Weiss, E., & Baty, D. (2009). Therapeutic antibodies: Successes, limitations and hopes for the future. *British Journal of Pharmacology*, *157*, 220–233.

Chen, X., Dudgeon, N., Shen, L., & Wang, J. H. (2005). Chemical modification of gene silencing oligonucleotides for drug discovery and development. *Drug Discovery Today*, *10*, 587–593.

van Deemter, J. J., Zuiderweg, F. J., & Klinkenberg, A. (1995). Longitudinal diffusion and resistance to mass transfer as causes of nonideality in chromatography. *Chemical Engineering Science*, *50*, 3869–3882.

Eble, J. E., Grob, R. L., Antle, P. E., & Snyder, L. R. (1987). Simplified description of high-performance liquid chromatographic separation under overload conditions, based on the Craig distribution model. III. Computer simulations for two co-eluting bands assuming a Langmuir isotherm. *Journal of Chromatography A*, *405*, 1–29.

Enmark, M., Bagge, J., Samuelsson, J., Thunberg, L., Örnskov, E., Leek, H., Limé, F., & Fornstedt, T. (2020). Analytical and preparative separation of phosphorothioated oligonucleotides: Columns and ion-pair reagents. *Analytical and Bioanalytical Chemistry*, *412*, 299–309.

Ginn, S. L., Amaya, A. K., Alexander, I. E., Edelstein, M., & Abedi, M. R. (2018). Gene therapy clinical trials worldwide to 2017: An update. *Journal of Gene Medicine*, *20*, 1–51.

Glennie, M. J., & Johnson, P. W. M. (2000). Clinical trials of antibody therapy. *Immunology Today*, *21*, 403–410.

Gold, L. (1995). Oligonucleotides as research, diagnostic, and therapeutic agents. *Journal of Biological Chemistry*, *270*, 13581–13584.

Golshan-Shirazi, S., & Guiochon, G. (1990). Theoretical explanation of the displacement and tag-along effects. *Chromatographia*, *30*, 613–617.

Gooding, M., Malhotra, M., Evans, J. C., Darcy, R., & O'Driscoll, C. M. (2016). Oligonucleotide conjugates—Candidates for gene silencing therapeutics. *European Journal of Pharmaceutics and Biopharmaceutics*, *107*, 321–340. https://doi.org/10.1016/j.ejpb.2016.07.024

Guiochon, G., & Ghodbane, S. (1988). Computer simulation of the separation of a two-component mixture in preparative scale liquid chromatography. *Journal of Physical Chemistry*, *92*, 3682–3686.

Guiochon, G., & Katti, A. (1987). Preparative liquid chromatography. *Chromatographia*, *24*, 165–189.

Ho, P. Y., & Yu, A. M. (2016). Bioengineering of noncoding RNAs for research agents and therapeutics. *Wiley Interdisciplinary Reviews: RNA*, *7*, 186–197.

Horvath, C., Nahum, A., & Franz, J. H. (1981). High-performance displacement chromatography. *Journal of Chromatography218*, 365–393.

Hoy, S. M. (2018). Patisiran: First global approval. *Drugs*, *78*, 1625–1631. https://doi.org/10.1007/s40265-018-0983-6

Jungbauer, A. (2013). Continuous downstream processing of biopharmaceuticals. *Trends in Biotechnology*, *31*, 479–492. https://doi.org/10.1016/j.tibtech.2013.05.011

Kalász, H. (2003). Displacement chromatography. *Journal of Chromatographic Science*, *41*, 281–283.

Kazutaka, N., Wenying, P., Kie, Y. -T., Yumiko, S., Tomoko, N., Tsuyoshi, Y., Keiko, N., Kotaro, Y., Hiroya, K., Hidenori, Y., Takeshi, B., Fumiko, O., Kanjiro, M., Koichi, M., Punit, P. S., Audrey, L., Masayuki, Y., Frank, C., Kazunori, B. O., …Takanori Y. (2016). DNA/RNA heteroduplex oligonucleotide for highly efficient gene. *Clinical and Experimental Neuroimmunology7*, 108–109.

Keam, S. J. (2018). Inotersen: First global approval. *Drugs*, *78*, 1371–1376. https://doi.org/10.1007/s40265-018-0968-5

Kim, J., Hu, C., Moufawad El Achkar, C., Black, L. E., Douville, J., Larson, A., Pendergast, M. K., Goldkind, S. F., Lee, E. A., Kuniholm, A., Soucy, A., Vaze, J., Belur, N. R., Fredriksen, K., Stojkovska, I., Tsytsykova, A., Armant, M., DiDonato, R. L., Choi, J., …Yu, T. W. (2019). Patient-customized oligonucleotide therapy for a rare genetic disease. *New England Journal of Medicine*, *381*, 1644–1652.

Kim, T. K., Botti, C., Angelo, J., Xu, X., Ghose, S., Li, Z. J., Morbidelli, M., & Sponchioni, M. (2021). Experimental design of the multicolumn countercurrent solvent gradient purification (MCSGP) unit for the separation of pegylated proteins. *Industrial & Engineering Chemistry Research*, *60*, 10764–10776.

Krättli, M., Müller-Späth, T., & Morbidelli, M. (2013). Multifraction separation in countercurrent chromatography (MCSGP). *Biotechnology and Bioengineering*, *110*, 2436–2444.

Luca, D. C., Felletti, S., Lievore, G., Chenet, T., Morbidelli, M., Sponchioni, M., Cavazzini, A., & Catani, M. (2020). Modern trends in downstream processing of biotherapeutics through continuous chromatography: The potential of multicolumn countercurrent solvent gradient purification. *TrAC, Trends in Analytical Chemistry*, 132.

Madabhushi, S. R., Gavin, J., Cutler, C., Chmielowski, R., Ray, W., & Chen, H., Quantitative Assessment of Environmental Impact of Biologics Manufacturing Using Process Mass Intensity Analysis. (2018). *Biotechnol Prog*, *34*, 1–8.

Morrison, C. (2019). Fresh from the biotech pipeline-2018. *Nature Biotechnology*, *37*, 118–123. https://doi.org/10.1038/s41587-019-0021-6

Müller-Späth, T., StröHlein, G., Lyngberg, O., & Maclean, D. (2013). Enabling high purities and yields in therapeutic peptide purification using multicolumn countercurrent solvent gradient purification. *Chimica Oggi/Chemistry Today*, *31*, 56–60.

Nelson, A. L., Dhimolea, E., & Reichert, J. M. (2010). Development trends for human monoclonal antibody therapeutics. *Nature Reviews Drug Discovery*, *9*, 767–774. https://doi.org/10.1038/nrd3229

Paredes, E., Aduda, V., Ackley, K. L., & Cramer, H. (2017). Manufacturing of oligonucleotides. Comprehensive Medical Chemistry III. 233–279. https://www.sciencedirect.com/science/article/pii/B9780124095472124230

Roberts, T. C., Langer, R., & Wood, M. J. A. (2020). Advances in oligonucleotide drug delivery. *Nature Reviews Drug Discovery*, *19*, 673–694. https://doi.org/10.1038/s41573-020-0075-7

Seidel-Morgenstern, A. (2004). Experimental determination of single solute and competitive adsorption isotherms. *Journal of Chromatography, A*, *1037*, 255–272.

Stein, C. A., & Castanotto, D. (2017). FDA-approved oligonucleotide therapies in 2017. *Molecular Therapy*, *25*, 1069–1075. https://doi.org/10.1016/j.ymthe.2017.03.023

Steinebach, F., Müller-Späth, T., & Morbidelli, M. (2016). Continuous counter-current chromatography for capture and polishing steps in biopharmaceutical production. *Biotechnology Journal*, *11*, 1126–1141.

Ströhlein, G., Aumann, L., Mazzotti, M., & Morbidelli, M. (2006). A continuous, counter-current multi-column chromatographic process incorporating modifier gradients for ternary separations. *Journal of Chromatography, A*, *1126*, 338–346.

Ulmer, N., Pfister, D., & Morbidelli, M. (2017). Reactive separation processes for the production of PEGylated proteins. *Current Opinion in Colloid & Interface Science*, *31*, 86–91.

Vogg, S., Müller-Späth, T., & Morbidelli, M. (2020). Design space and robustness analysis of batch and counter-current frontal chromatography processes for the removal of antibody aggregates. *Journal of Chromatography, A*, *1619*, 12–14.

Yin, W., & Rogge, M. (2019). Targeting RNA: A transformative therapeutic strategy. *Clinical and Translational Science*, *12*, 98–112.

El Zahar, N. M., Magdy, N., El-Kosasy, A. M., & Bartlett, M. G. (2018). Chromatographic approaches for the characterization and quality control of therapeutic oligonucleotide impurities. *Biomedical Chromatography*, *32*, 32.

SUPPORTING INFORMATION

Additional supporting information can be found online in the Supporting Information section at the end of this article.

How to cite this article: Fioretti, I., Müller-Späth, T., Weldon, R., Vogg, S., Morbidelli, M., & Sponchioni, M. (2022). Continuous countercurrent chromatographic twin-column purification of oligonucleotides: The role of the displacement effect. *Biotechnology and Bioengineering*, 119, 1861–1872. https://doi.org/10.1002/bit.28093